An automated system using spatial oversampling for optical mapping in murine atria. Development and validation with monophasic and transmembrane action potentials

Yu, Ting Yue; Syeda, Fahima; Holmes, Andrew P; Osborne, Benjamin; Dehghani, Hamid; Brain, Keith L; Kirchhof, Paulus; Fabritz, Larissa

DOI:
10.1016/j.pbiomolbio.2014.07.012

Progress in Biophysics and Molecular Biology 115 (2014) 340–348

Contents lists available at ScienceDirect

Progress in Biophysics and Molecular Biology

journal homepage: www.elsevier.com/locate/pbiomolbio

Original research

An automated system using spatial oversampling for optical mapping in murine atria. Development and validation with monophasic and transmembrane action potentials

Ting Yue Yu [a, b], Fahima Syeda [a], Andrew P. Holmes [a], Benjamin Osborne [a], Hamid Dehghani [b, c], Keith L. Brain [d], Paulus Kirchhof [a], Larissa Fabritz [a, *]

[a] Centre for Cardiovascular Sciences, School of Clinical and Experimental Medicine, College of Medical and Dental Sciences, University of Birmingham, UK
[b] Doctoral Training Centre for Physical Sciences of Imaging in the Biomedical Sciences (PSIBS), University of Birmingham, UK
[c] School of Computer Science, College of Engineering and Physical Sciences, University of Birmingham, UK
[d] School of Clinical and Experimental Medicine, College of Medical and Dental Sciences, University of Birmingham, UK

ARTICLE INFO

Article history:
Available online 15 August 2014

Keywords:
Optical mapping
Murine model
Isolated atrium
Conduction velocity
Atrial action potential duration
Atrial fibrillation

ABSTRACT

We developed and validated a new optical mapping system for quantification of electrical activation and repolarisation in murine atria. The system makes use of a novel 2nd generation complementary metal-oxide-semiconductor (CMOS) camera with deliberate oversampling to allow both assessment of electrical activation with high spatial and temporal resolution (128 × 2048 pixels) and reliable assessment of atrial murine repolarisation using post-processing of signals. Optical recordings were taken from isolated, superfused and electrically stimulated murine left atria. The system reliably describes activation sequences, identifies areas of functional block, and allows quantification of conduction velocities and vectors. Furthermore, the system records murine atrial action potentials with comparable duration to both monophasic and transmembrane action potentials in murine atria.

1. Introduction

Atrial fibrillation is the most common sustained arrhythmia in man and a common cause of stroke and cardiac deaths. Although good progress has been made in the characterisation of factors that cause AF (Camm et al., 2012a,b; Schotten et al., 2011; Wakili et al., 2011), there is still an unmet need for better therapies to prevent incident and recurrent AF (Camm et al., 2012a,b; Kirchhof et al., 2013). Unravelling the mechanisms conveying the genetic basis of atrial fibrillation (Benjamin et al., 2009; Ellinor et al., 2012; Gudbjartsson et al., 2007) is a promising and relatively new avenue to novel preventive and therapeutic targets. Genetically altered murine models are popular tools for the study of molecular disease mechanisms, including of atrial fibrillation. Such models allow the characterisation of the functional and molecular consequences of defined genetic alterations, thereby allowing us to identify arrhythmia mechanisms attributable to such modifications. This type of research extends the association studies in patients and populations which are limited by comorbidities, ethical restraints and low sample availability (Riley et al., 2012). The small size of murine hearts, particularly the atria, poses a challenge for detailed electrophysiological assessment, and especially for high density mapping of electrical activation and repolarisation. Evolving knowledge of existence of regional heterogeneities calls for the development of a technique with high spatial resolution, so that the extent of heterogeneity can be identified (Di Diego et al., 2013; Waldeyer et al., 2009). Additionally, the high frequency and fast repolarisation properties of the murine atrium necessitate high temporal resolution.

Optical mapping is an established technique for high spatial and temporal resolution non-contact investigation of electrical excitability of cardiac cells, tissues and whole organs (Efimov et al., 1994; Lee et al., 2011; Rohr and Salzberg, 1994; Salama et al., 1987; Wu et al., 2001). Optical mapping of cardiac tissue uses voltage-sensitive dyes to visualise action potentials as changes in

Abbreviations: ADC, Analogue to digital converter; AF, Atrial fibrillation; APD, Action potential duration; CL, Cycle length; CMOS, Complementary metal-oxide-semiconductor; CV, Conduction velocity; LA, Left atrium; LED, Light emitting diode; MAP, Monophasic action potential; OAP, Optical action potential; SEM, Standard error of the mean; TAP, Transmembrane action potential; TIFF, Tagged image file format.

* Corresponding author. Centre for Cardiovascular Sciences, School of Clinical and Experimental Medicine, College of Medical and Dental Sciences, University of Birmingham, Edgbaston, Birmingham B15 2TT, UK. Tel.: +44 (0)121 414 6938.
E-mail address: L.Fabritz@bham.ac.uk (L. Fabritz).

http://dx.doi.org/10.1016/j.pbiomolbio.2014.07.012

fluorescence, as an index for changes in transmembrane potentials (Salzberg et al., 1973). Numerous improvements have been made to overcome technical difficulties associated with optical mapping of cardiac tissue including removal of contraction artefacts in large and small vertebrates by using uncouplers (Dou et al., 2007; Fedorov et al., 2007; Jou et al., 2010; Wu et al., 1998) and sensitive optical dyes (Efimov and Fahy, 1997; Ehrenberg et al., 1987; Rohr and Salzberg, 1994). As such, this technique has provided important insights into the mechanisms of atrial arrhythmias in murine models (Arora et al., 2003; Blana et al., 2010; Kirchhof et al., 2011a,b). The complex electrophysiology of atrial fibrillation (Eckstein et al., 2013; Kirchhof et al., 2011a,b; Verheule and Tuyls, 2013), renders a higher spatial resolution of murine atrial activation and repolarisation mapping technology desirable. This allows us to pinpoint further, the regional origins and patterns of AF activation (Mandapati et al., 2000). Several foci of AF activation have already been identified in genetically altered mouse models (Benes et al., 2014; Faggioni et al., 2014). However, even with the best available systems, the need for higher spatial and temporal resolution combined with the small signal amplitude generated in the thin atrial murine tissue still poses technical challenges.

To further improve temporal and spatial resolution in cardiac optical imaging of murine atrial tissue, a second-generation complementary metal-oxide-semiconductor (CMOS) camera is utilised and novel algorithms developed to record and analyse atrial activation and repolarisation in the isolated, perfused murine atrium at high spatial resolution. A spatial oversampling technique is implemented to generate high-resolution activation maps at the same time as high quality repolarisation information. The algorithms used to generate isochronal maps and to perform APD measurements are largely automated to limit user bias and to facilitate high throughput analysis. Atrial optical action potentials are compared with epicardial atrial monophasic action potentials and atrial microelectrode transmembrane action potentials from isolated hearts to validate the findings.

2. Methods

2.1. Heart isolation

All surgical procedures were performed according to the Animals (Scientific Procedures) Act, 1986 and were approved by the Home Office and the local authorities. Hearts were rapidly excised by thoracotomy from WT adult mice (3–7 months old), on a 129/Sv or MF1 background, under terminal anaesthesia (200 mg/kg pentobarbital sodium) administered by intraperitoneal injection.

2.2. High resolution mapping using novel methods of automated data processing

Following isolation, hearts were mounted on a vertical Langendorff apparatus (Hugo Sachs, Germany) and the aorta retrogradely perfused with a standard bicarbonate buffered Krebs–Henseleit solution (see below), containing the voltage sensitive dye Di-4-Anepps (50 μM; Biotium, California, USA) and the excitation-contraction uncoupler blebbistatin (5 μM; Cayman Chemical, Michigan, USA), a well-characterised substance used for optical mapping (Fedorov et al., 2007; Kirchhof et al., 2011a,b). The dye was stored in 25 μl aliquots of 5 mg/ml. For each experiment an aliquot was mixed with 1 ml of Krebs solution and injected through a bolus port in the Langendorff system over a period of 5 min. The flow rate of the Krebs solution was kept at 4 ml/min and at 36 °C. After 5 min of infusion, the atria were dissected and placed in a superfusion chamber for image acquisition. A summary of the system set-up used for image acquisition is shown in Fig. 1. Preparations were continuously superfused with Krebs and blebbistatin to reduce contraction and paced incrementally (300 ms–80 ms paced cycle length) via platinum electrodes placed in the tissue bath at twice the diastolic voltage threshold at 2 ms pulse width. Stimuli were generated using an isolated constant voltage stimulator (Digitimer, UK) driven by an analogue to digital converter with spike2 software (Cambridge Electronic Design, UK). The atria were field illuminated by two twin LEDs at 530 nm (Cairn Research, UK). These were required to provide sufficient field illumination from all angles. A lens with a high numerical aperture (Schneider Kreuznach Xenon 0.95/25, NA = 0.52) was used to collect as many photons as possible. Wide field macroscopic images of emitted fluorescence (630 nm) were captured at a sampling frequency of 1 or 2 kHz using a novel, high speed, high resolution camera (128 × 2048 pixels, single pixel area: 6.5 μm by 6.5 μm, ORCA flash 4.0; Hamamatsu, Japan, Figs. 1 and 2). The camera reads the data from the centre of the sensor. Temporal resolution can be increased with reduced spatial resolution only in the vertical direction, as a trade-off. This allows for the full window of the sensor to be used in the horizontal direction. To reduce the read noise of the camera, the 4 × 4 binning option was used (Fig. 2B and C).

Images were extracted and collated using WinFluor V3.4.9 (Dr John Dempster, University of Strathclyde, UK) so that the fluorescence intensity from a specific region of interest (4 × 4 pixels) could be viewed as a single continuous waveform. This permitted the identification and monitoring of a greater number of optical action potentials (OAPs) across the entire surface of the mouse atrium at high spatial resolution. In addition, selected images could be exported into uncompressed Tagged image file format (TIFF) for the generation of whole atrial isochronal activation maps.

For the analysis of OAPs and generation of isochronal activation maps, data were automatically processed using custom made algorithms produced in MATLAB. For measurements of action potential duration (APD), an initial sign change was necessary as the emitted fluorescence intensity is inversely proportional to transmembrane voltage (Loew, 1996). Baseline subtraction was achieved by applying a 'linear top hat filter' to remove any fluorescence drift. At each cycle length, a maximum of 25 action potentials were averaged to calculate the mean action potential waveform for a selected region of interest (Fig. 1B). Previously we found that 25AP signals were sufficient to measure APD reliably. Fewer than 25 APs could be used, but this was dependent on the signal quality from each experiment. For example, a very good signal would require less averaging, but to keep the algorithm consistent 25 signals were routinely used. The baseline (100% repolarisation) was determined as the mean fluorescence signal recorded over 10 ms prior to depolarisation. The point of activation was defined as the peak rate of change (dF/dtmax) and APD30, 50 and 70, were evaluated by measuring the time from dF/dtmax to 30%, 50% and 70% repolarisation respectively (Fig. 1B). For each APD, the value usually falls between sampling time points, 1 ms apart for 1000 fps, 0.5 ms for a 2000 fps. The repolarisation time was estimated by connecting these two closest sampling time points above and below with straight lines. A simple linear equation can be used to determine the time for each APD.

Isochronal activation maps were produced after initially cropping the exported image stack to isolate the region of interest; this was the only step that required user input. Fluorescence intensity from every pixel was automatically analysed in the z (time) axis. The background was removed and signals were smoothed and then filtered using a Savitzky–Golay filter, a moving average filter which preserves signal morphology (Bachtel et al., 2011; Savitzky and Golay, 1964). Signals were differentiated to detect the time of activation, which was repeated until a 2D array (image) was compiled with each element (pixel) corresponding to a specific

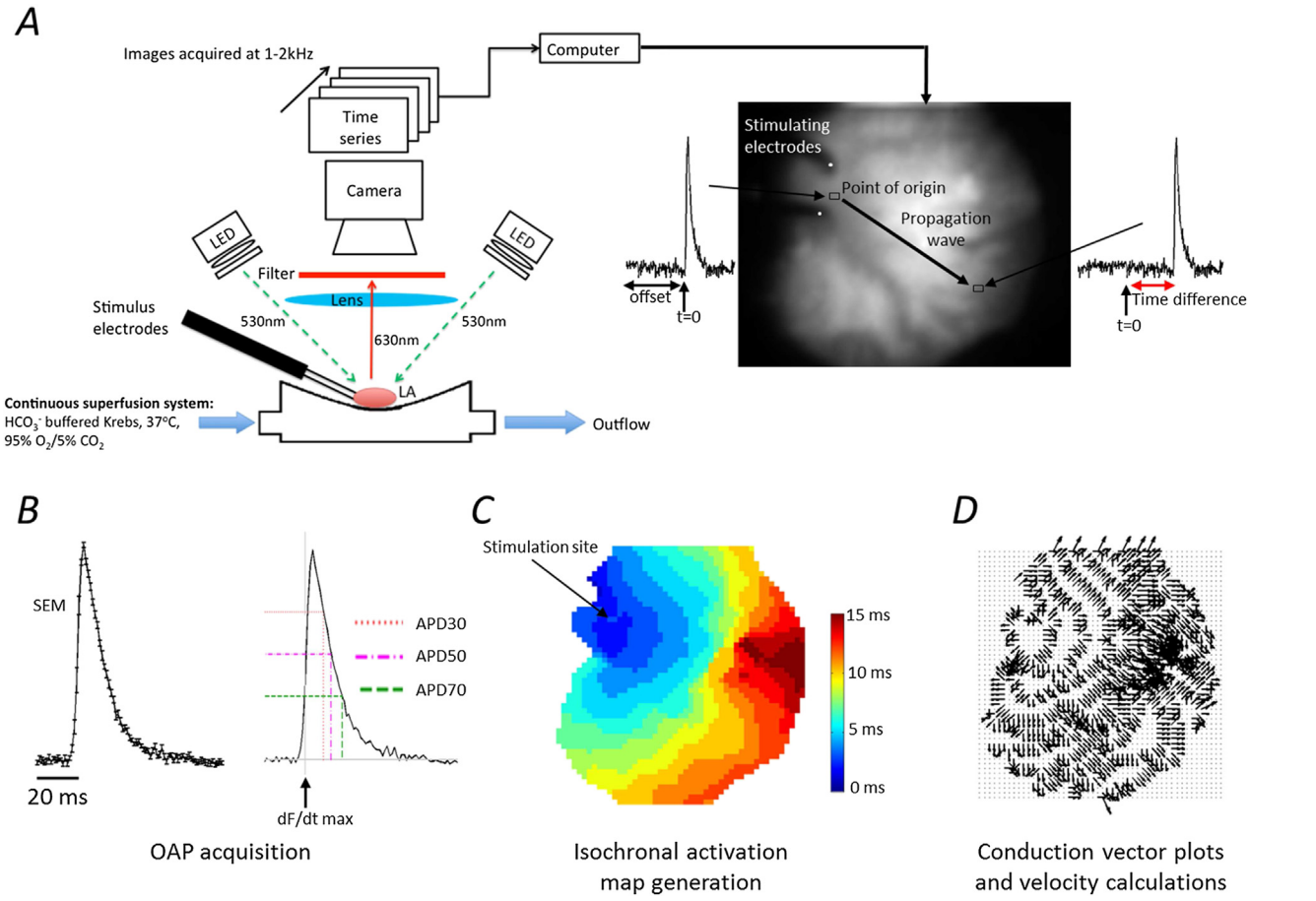

Fig. 1. Summary of the high resolution optical mapping system with automated analysis. **A** represents the schematic of the optical mapping system. The LA samples were excited by four 530 nm LEDs, and filtered through a high NA objective and a 630 nm long pass filter. The electrodes were used for programmed stimulation at 300–80 ms pacing cycle lengths. Images were captured at a frame rate of 1000–2000 per second and recorded on a desktop computer for analysis using Winfluor software. The images above were recorded at 1000 frames per second. The electrodes can be seen on the upper left of the atrial image with the line of activation indicated by the black arrow. The action potentials indicate the time at which the signals have reached that region. **B** This displays the outcome of an averaged signal taken from the left atrium stimulated at 100 ms CL (with standard errors. Adjacent, is the same signal with its action potential durations labelled at APD30, 50 and 70 with the start of activation indicated by dF/dtmax shown. **C** The isochronal map is a colour scale of the time taken to activate at each pixel, from the same atrium as above at 100 ms CL. The time increases in the direction opposite to where the electrodes are placed. **D** Conduction vectors that indicate the direction of the wave are generated from the activation map.

time. The origin of the activation wave was offset to zero ($t = 0$; Fig. 1C). All other time values in relation to the origin could be calculated (Fig. 1C) and then presented in the form of an isochronal map.

For assessment of conduction velocities, the pixel size was measured to be 71 μm and as each pixel represents a time value, the velocity can be measured. The isochronal maps were generated as mentioned above, with each time zone represented with a different colour. From these maps the contours of the wave of propagation were easily interpreted. To ensure accuracy, measurements were always made perpendicular to the wavefront. Two points across several 'time zones', usually a minimum of three, were selected. From the distance and the difference in time between those points, velocity was calculated in cm/second.

2.3. Monophasic action potentials

The new optical mapping system was validated by comparing activation and repolarisation time with two established methods, monophasic action potentials (MAP) (Blana et al., 2010; Kirchhof et al., 2011a,b), and transmembrane action potentials obtained in the same atrial preparations. Briefly, for MAP acquisition, published techniques (Blana et al., 2010; Kirchhof et al., 2011a,b; Knollmann et al., 2001) were employed and MAP recordings were obtained in the intact, perfused heart immediately prior to dissecting the atria for optical mapping. Whole hearts were cannulated and mounted on a vertical Langendorff apparatus (Hugo Sachs, Germany) and retrogradely perfused with standard bicarbonate buffered Krebs–Henseleit solution at 36–37 °C, at constant perfusion pressure (100 ± 5 mmHg) and coronary flow (4 ± 0.5 ml/min). A 2.0 French octapolar mouse electrophysiological catheter with electrodes sized 0.5 mm and spaced at 0.5 mm (CIB'ER MOUSE, NuMED, LLC., N.Y., USA) was inserted into the right atrium for pacing (120 ms–80 ms, 2 ms pulse width). Stable left atrial MAP recordings were obtained using a miniaturised MAP catheter mounted on spring-loaded electrode holder. Voltage signals were amplified, digitised and viewed on a PC loaded with iox2 software (EMKA, France). Measurements of action potential duration (APD) and inter-atrial activation times were acquired using algorithms generated in iox2.

2.4. Transmembrane action potentials

Transmembrane murine atrial action potentials (TAP) were recorded as published (Lemoine et al., 2011) immediately before or after the optical mapping procedure. TAPs were recorded from

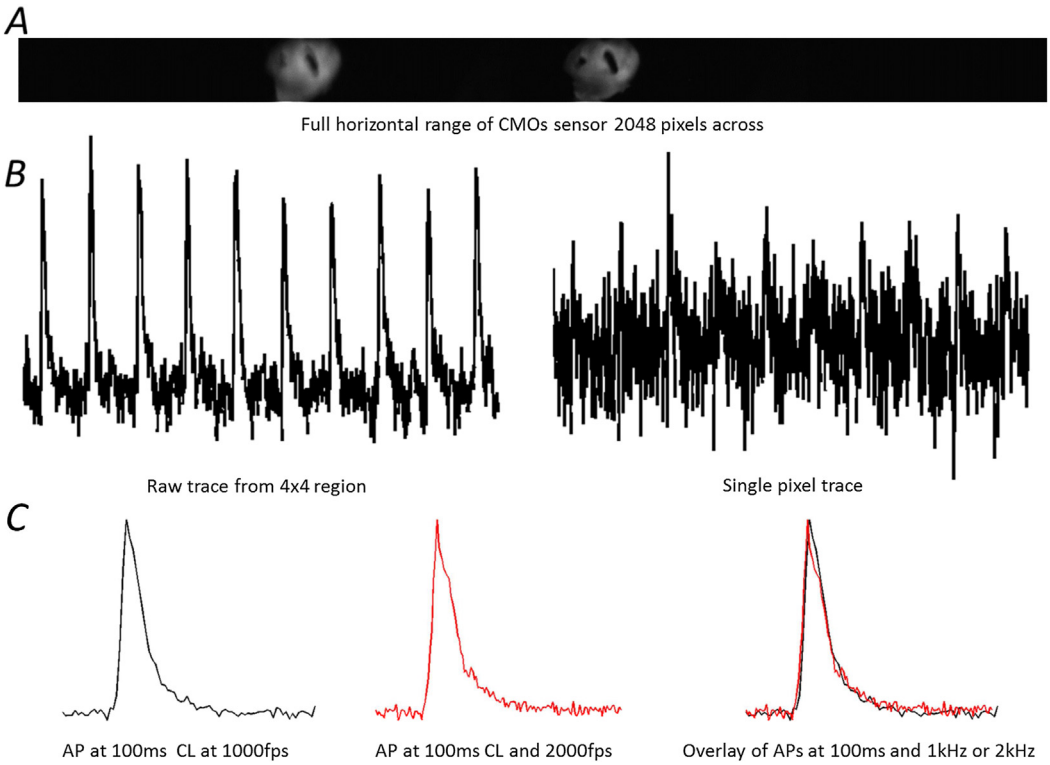

Fig. 2. Examples of raw data from different acquisition techniques. **A** Raw image of the left atria from the ORCA Flash 4.0. Two images can be seen as an image splitter from two different wavelengths focused on the single sensor. Resolution shown here is at 128 × 2048 pixels. **B** Raw traces from the left atria over a period of 1 s showing 10 action potentials. There is less noise in the region of measurement using 4 × 4 pixels (left) compared to single pixels which show very little information, with the action potentials barely visible (right). **C** Comparison of two action potential signals normalised to lie between 0 and 1 taken at 100 ms cycle length (CL) of the same atria and same region of interest but at different acquisition speeds. These signals showed very minute variation in signal as we can see in the overlay.

isolated superfused LA samples prepared as above using borosilicate glass microelectrodes (tip resistance 15–30 MΩ), filled with 3 M KCl. Voltage signals were amplified (Axoclamp 2B; Molecular Devices, USA), digitised and displayed using spike2 software (Cambridge Electronic Design, UK). The sampling frequency was 20 kHz. Preparations were paced successively (300 ms–80 ms) with platinum electrodes at twice the diastolic voltage threshold, with a minimum of 50 APs recorded at each cycle length using an isolated constant voltage stimulator (Digitimer, UK) driven by an analogue to digital converter with Spike2 software (Cambridge Electronic Design, UK). Measurements of APD and intra-atrial activation times were obtained using custom-made spike2 algorithms.

2.5. Solutions

For all experiments a standard bicarbonate buffered Krebs–Henseleit solution was used containing in mM: NaCl 118; $NaHCO_3$ 24.88; KH_2PO_4 1.18; Glucose 5.55; Na-Pyruvate 5; $MgSO_4$ 0.83; $CaCl_2$ 1.8; KCl 3.52, equilibrated with 95% O_2 and 5% CO_2 and heated to 36–37 °C. Under these conditions the pH was maintained at 7.4. For experiments with 1 μM flecainide, the drug was added to the superfusate and circulated for 15 min to reach steady state (Blana et al., 2010) before capturing images.

2.6. Data analysis

Values are expressed as mean ± standard error of mean unless otherwise stated. Statistical analysis was performed using one way Analysis of Variance (ANOVA) with Bonferroni or Dunnett's post hoc analysis where appropriate (GraphPad Prism 5.01). Significance was taken as $p < 0.05$.

3. Results

After development and optimisation of the setup, the quality of OAP recordings was sufficient for generating isochronal maps for conduction measurements from an initial 5/10 to currently 8/10 of the hearts used due to quality criteria, while basic action potential duration measurements could be acquired from all hearts. For a data set to meet the criteria for conduction measurements, the isochronal maps must show a clear direction of wavefront propagation. This allowed for the selection of two points across several 'time zones' for calculation of conduction velocity.

3.1. Optical action potentials

As for TAPs and MAPs, the optically generated action potentials were characterised by a fast depolarisation and a slower repolarisation. The baseline correction adjusted the signal allowing for OAP measurements in all preparations with accuracy (Fig. 3A). Combining several of the oversampled regions, up to four pixels were occasionally required to achieve sufficient signal-to-noise ratios for precise determination of the repolarisation phase of the action potential. OAPs measured using this novel oversampling method exhibited similar morphology and duration characteristics when compared with those recorded using more standard electrophysiology techniques (Fig. 3B and C). At 300 ms CL OAPs at APD50 were 10.9 ± 0.9 ms and APD70 14.7 ± 1.2 ms and showed no

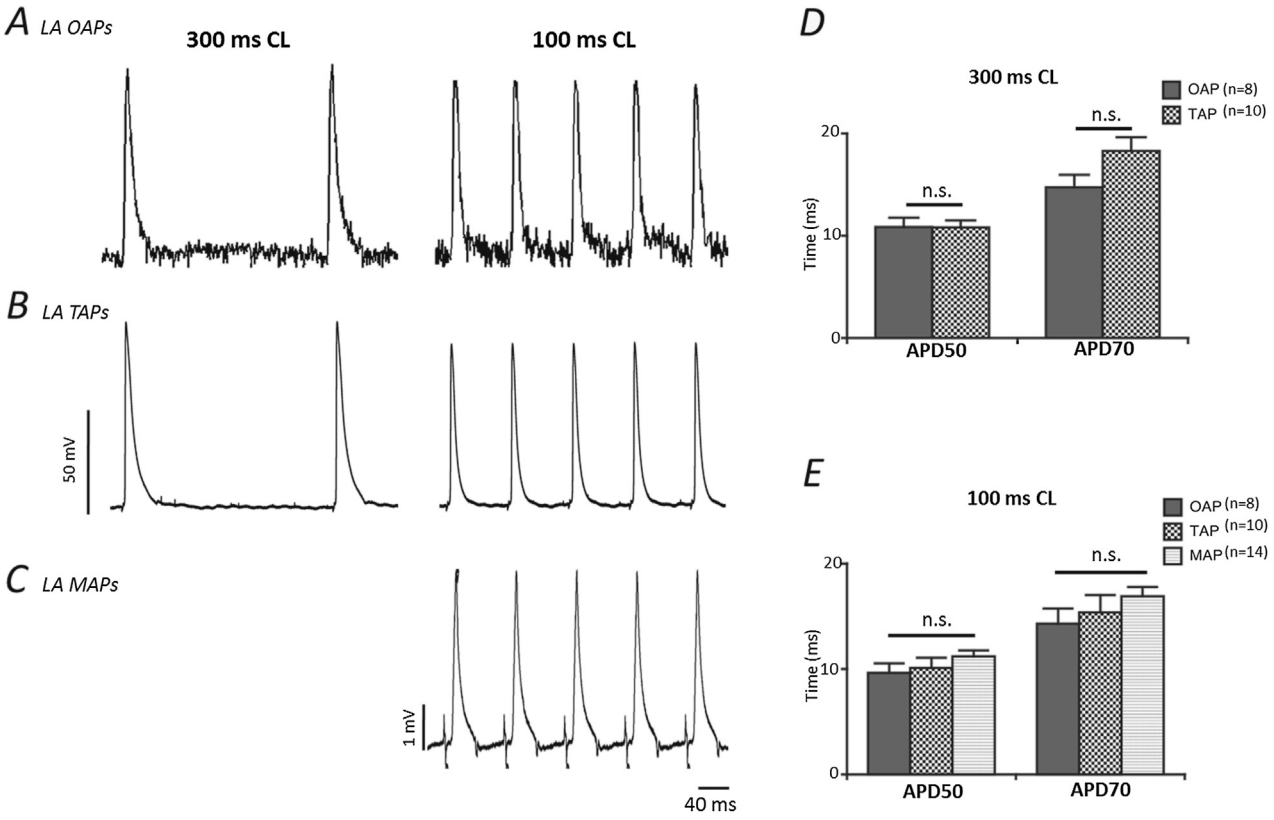

Fig. 3. Comparison of action potentials obtained using the high resolution optical system with other standard electrophysiological techniques. Characteristic raw trace examples of LA (left atrium). **A** optical action potentials (OAP) acquired at 1 kHz. **B** transmembrane (TAP); and **C** monophasic (MAP) action potentials recorded at cycle lengths of 300 ms and 100 ms. **D** and **E** Grouped data showing consistency of optical action potential durations at 50% and 70% repolarisation compared with TAPs and MAPs at 300 ms and 100 ms cycle lengths respectively. Error bars indicate + SEM. Data presented is from 8 regions of interest (ROI) from 8 LAs (OAPs), 10 cells from 5 LAs (TAPs) and 14 recordings from 14 LAs (MAPs).

difference from TAPs at 300 ms cycle lengths (10 cells, 5 atria, Fig. 3D). In another set of experiments, MAPs were recorded from the intact, beating heart just prior to dissection of atrial tissue for OAP measurement. We did not detect a significant difference in APD50 or APD70 between OAPs (9.6 ± 0.9 ms and 14.3 ± 1.4 ms respectively) and TAPs and MAPs at a more physiological paced cycle length of 100 ms ($n = 14$, Fig. 3E). This degree of uniformity therefore suggests that OAPs obtained using this technique can be used to make accurate and reliable assessments of APDs in the mouse atria.

3.2. Activation maps and conduction velocities

Example isochronal activation maps generated at different cycle lengths for the entire LA are shown in Fig. 4A and demonstrate in greater detail an obvious slowing of the activation spread at shorter cycle lengths. Accordingly, atrial conduction times, measured from the time point of stimulation to the fastest upstroke of the TAP (Fig. 4B) or MAP (Fig. 4C) were prolonged at 100 ms and 80 ms cycle lengths. Fig. 4D illustrates the recording positions of TAP and MAP with respect to the stimulation site. Fig. 4E gives mean conduction velocities (CV), measured with the new optical mapping setup, and throughout the entire left atrium at different paced cycle lengths. CV drops at higher paced cycle length, as expected (CV: 43.0 ± 1.3 cm/s–22.0 ± 4.7 cm/s from 300 ms to 80 ms CL respectively). Fig. 4F illustrates the parallel increase in atrial activation times measured by TAP (left atrial stimulation to mid-LA recording site) and by MAP (right atrial septal stimulation to distant LA recording site). Due to the higher intrinsic rate of the intact, beating heart (including the right atrium and the sinus node), MAP recordings were not available at 300 ms paced cycle length.

When adding the sodium channel blocker flecainide to the superfusion (1 μM), we observed an expected slowing in atrial conduction spread (Fig. 5A and B). The isochronal maps clearly demonstrate that flecainide superfusion produces a well-defined region of functional conduction block in the mid-to inferior left atrium, disturbing the normal pattern of electrical propagation, severely prolonging activation time in certain areas and potentially predisposing to re-entrant arrhythmia (see supplementary video file; Fig. 5B).

Supplementary video related to this article can be found at http://dx.doi.org/10.1016/j.pbiomolbio.2014.07.012.

Thus, in summary, our setup reliably reflects physiological changes in atrial activation and visualises the propagation of electrical activation waves across the entire murine left atrium, as well as allowing for accurate calculation of APD and intra-atrial conduction velocity at any defined region. In addition, this optical mapping system can be used to more definitively trace disordered electrical conduction in the mouse atrium, potentially induced by pharmacological agents, genetic manipulation or features common in certain models of pathology such as heart failure.

4. Discussion

4.1. Main findings

A novel system for optical mapping of electrical activation and repolarisation in the murine atrium is described. The system makes use of new imaging technology, namely a high-resolution 2nd generation CMOS camera, to achieve high temporal and spatial resolution of electrical activation and repolarisation in the murine atrium. It is demonstrated that recording is feasible using

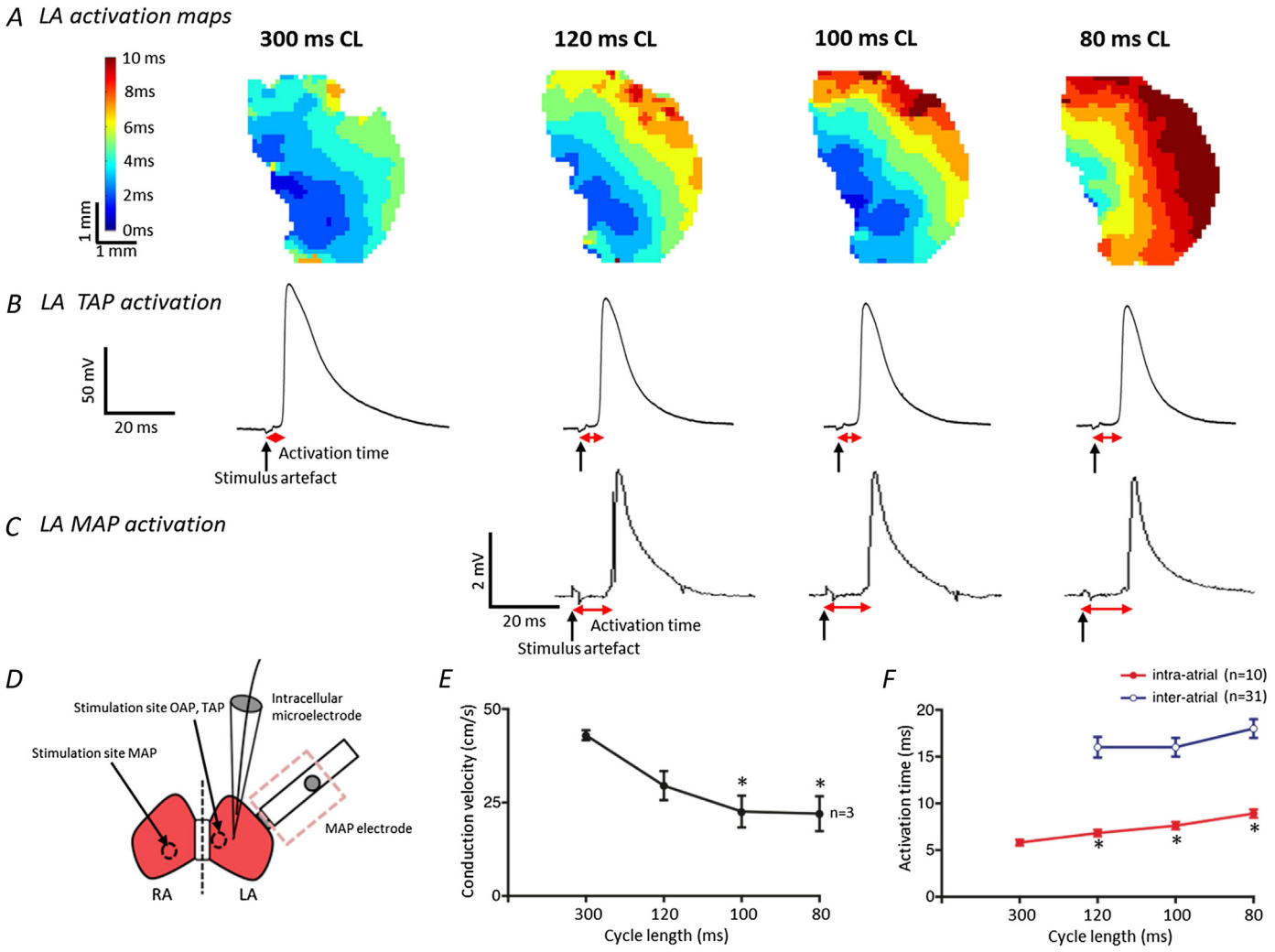

Fig. 4. Activation wave propagation across the murine left atrium and conduction velocities at different pacing cycle lengths. **A** Examples of the activation spread across the same left atrium at different cycle lengths as recorded by the new optical mapping system at 1 kHz. The high resolution isochronal maps indicate that at shorter cycle lengths the activation time across the whole tissue is increased. A similar, but less detailed, pattern of delayed activation at shorter cycle lengths is shown using recordings of **B** TAPs and **C** MAPs, as evidenced by the increase in time from the stimulus artefact to the point of activation (Vmax). **D** A schematic of the atria showing the stimulus and recording sites for the three techniques. When using optical mapping the whole left atrium is imaged and stimulated towards the septum. For TAP recordings the stimulation site is the same but the recording site is approximately in the centre of the tissue. Epicardial left atrial MAP signals were recorded from the intact whole heart and stimulated at the endocardial surface of the right atrium with the octapolar catheter. **E** Mean conduction velocities at different cycle lengths, $n = 3$ LA. Error bars indicate ± SEM, * denotes $P < 0.05$ compared with velocity at 300 ms CL; one way repeated measures ANOVA with Dunnett's post hoc analysis. **F** TAP and MAP activation times at decreasing cycle lengths. Data presented is from 10 cells from 5 LAs (TAPs) and 31 recordings from 31 LAs (MAPs). Error bars indicate ± SEM, * denotes $P < 0.05$ compared with activation time at 300 ms CL; one way ANOVA with Dunnett's post hoc analysis.

the system and shown that the measurements yield comparable action potential waveforms and action potential durations when compared to monophasic and transmembrane atrial action potentials. Furthermore, it is shown that the system is capable of detecting changes in conduction velocity and functional conduction block. In our hands, the oversampling of recordings allows us to maximise the information collected in each experiment, as a higher spatial resolution is conducive to the detection of small activation changes, while larger sampling areas are acceptable for the assessment of atrial repolarisation, where a higher signal to noise ratio may be needed to accurately determine action potential duration. In addition to this, the algorithms used are useful in reducing the time needed for a user to analyse APD measurements and produce activation maps. For example, to correct for baseline shifts, it is common to fit a linear or polynomial equation to the signal (Laughner et al., 2012). In our experiments, these baseline shifts were extremely variable. We therefore had to use a different approach to existing correction methods. Here we use a common top hat filter normally applied to 2D quality images but on a 1D signal on our action potentials. Another example is the detection of $t = 0$ on the isochronal maps. It is a useful tool for speeding up analysis and again, for limiting user bias.

Assessment of murine atrial electrophysiology is an essential tool to understand the functional consequences of defined genetic modifications, including complex gene expression changes e.g. secondary to altered function of transcription factors (Kirchhof et al., 2011a,b; Riley et al., 2012; Wang et al., 2010), or the effects of inhibitory or regulatory RNA molecules. Environmental factors like the effect of training, interventions and chronic or acute drug treatment (Fabritz et al., 2010, 2011) can be assessed with the increased number of pixels in this system in the future, including larger and irregular specimens. The increased spatial resolution in this system will also allow us to identify heterogeneities within the tissue. Imaging of murine embryos should also be possible with this system (Benes et al., 2014).

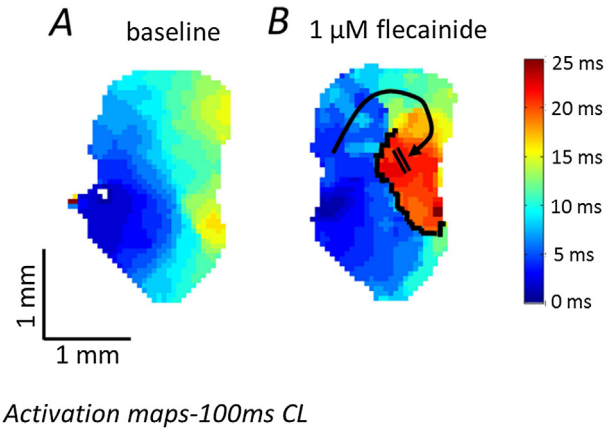

Fig. 5. Functional conduction block (induced by flecainide) in the murine left atrium. **A** Characteristic activation spread across the left atrium under control conditions, taking approximately 15 ms to traverse the whole tissue when paced at 100 ms CL. **B** Disrupted activation wave propagation across the same left atrium following 15 min of 1 µM flecainide infusion. A clearly defined region of functional conduction block develops and is outlined in black. An alternative route of conduction (black arrow) is required and this causes a substantial increase in activation time (25 ms). Both images acquired at 1 kHz sampling.

By building an optical mapping system around a novel 2nd generation oversampling high-resolution CMOS camera with high light sensitivity, we were able to record electrical activation and repolarisation with high accuracy and reliability, yielding information that reflects murine atrial biology (Figs. 2–4). The ORCA camera has very recently been used and shown to capture action potentials in spontaneously spiking HEK cells (Park et al., 2013). Signals from HEK cells occur at approximately 3 APs per second. The pacing rate applied in our experiments in live intact organ tissue was much higher and represented a higher challenge to the camera resolution. The validation data suggest that the system can reliably record atrial repolarisation, making it attractive for the study of arrhythmia mechanisms in genetically altered murine models that mimic inherited arrhythmogenic diseases and/or replicate common gene expression changes associated with common cardiac diseases.

4.2. Technical considerations

Optical mapping of mouse hearts has been used to characterise arrhythmia mechanisms since the beginning of this century. Initially, systems were developed to measure ventricular activation and repolarisation (Baker et al., 2000; Brunner and Kodirov, 2003), and more recently expanded to atrial preparations (Glukhov et al., 2010; Kirchhof et al., 2011a,b; Verheule et al., 2004). One of the most commonly used systems is the custom-made SCIMEDIA system that provides a 100 × 100 pixel field at high temporal resolution (Bezzina et al., 2013; Kirchhof et al., 2011a,b). Especially at high sampling rates, the relatively low signal strength generated by the thin murine atrial tissue has been a challenge. The system developed and validated here uses emerging technology, i.e. a 2nd generation CMOS camera capable of detecting low amplitude light signals at superior spatial resolution (128 × 2048 pixels) and good temporal resolution (1–2 kHz). A higher temporal resolution is needed when capturing quick cellular changes, e.g. action potential depolarisation. A higher spatial resolution is desirable when trying to precisely locate phenomena changing at a lower rate. With this resolution span, each individual pixel provides a signal with a relatively low signal to noise ratio, due to the limited number of light emitting events of the recorded tissue. The spatial oversampling of the signals during data acquisition allows the post-processing of signals to optimise the information per pixel. Specifically, a high spatial resolution is used to assess atrial activation with optimal accuracy and an acceptable signal to noise ratio. The employed algorithm for correction of baseline fluctuation was robust to all types of – sometimes random – changes in baseline fluorescence, thus increasing the reliability of the measurements and the yield of analysable experiments. Reliable assessment of repolarisation, in contrast, was possible using combination of individual signals in the analysis phase, thereby sacrificing some of the spatial resolution, and by signal averaging during steady state pacing. Thus, the proposed new, versatile system allows the adjustment of image parameters after the end of the experiment to suit specific analysis needs, therefore increasing the information yield from each experiment.

This system was capable of recording valid action potential waveforms over a wide range of paced cycle lengths, and with simultaneous recording of action potential durations from all regions of the left atrium. Using the post-processing methods described above, this system will provide detailed insights into the regional differences in atrial action potential duration, and their change in genetically modified models.

The preparation used here was stable over experimental protocols of 1–1.5 h duration, demonstrating that superfusion of the murine atrium is adequate to maintain the integrity of the superfused atrium during acute interventions such as antiarrhythmic drugs (Fig. 5) at bradycardic and physiological cycle lengths. Automated analysis of APD and activation patterns is another important feature of the present system. Semi-automated procedures, involving the investigator in the initial selection of suitable recording periods and in the definition of suitable regions of interest for assessment of repolarisation, combined with automated post-processing of such signals, allows valid, investigator-controlled yet rapid and high-throughput recordings of electrical activation and repolarisation in the intact murine atrium.

4.3. Limitations and further developments

The new optical mapping system can be used to characterise the electrophysiological behaviour of murine atrial tissue in sufficient detail to describe arrhythmogenic changes in electrical activation and repolarisation in murine atria. The isolated superfused, dye-loaded atrium is sufficiently stable to allow the assessment of acute effects of pharmacological interventions such as antiarrhythmic drugs or miRNAs. Cross-over designs, e.g. giving a substance initially and observing the reverse effect during wash out (Blana et al., 2010), can be used in the future to demonstrate stability of the preparation even better. As such, it will be useful to describe arrhythmia mechanisms in genetically modified mice (Riley et al., 2012), especially when paired experiments in genetically modified and wild type mice are done in direct sequence, maintaining blinding during the analysis. The system was stable in assessing a cycle length of 100 ms for several minutes, but for even higher heart rates, a perfusion system would be beneficial to adjust for increased metabolic demand. Assessment of APD needed an uncoupler, but assessment of conduction velocity might be possible without an uncoupler in the near future by filtering techniques following the sharp upstroke of the action potential. Working without an uncoupler physiologically is an advantage especially if working with models of mechano-electrical feedback (Fabritz et al., 2012, 2011; Kohl et al., 1999).

This system seems capable of detecting regional differences in activation (Figs. 4 and 5) and repolarisation (illustrated by the capability to measure action potential duration at one single site in all experiments). The semi-automated analysis combined with the

high and adjustable spatial resolution will allow the generation of regional information quickly and reliably. The software can be further automatised, and source data made compatible with existing analysis platforms for optical activation maps and repolarisation shapes to ensure transferability of the results, ideally in an open access development process. Future developments may make use of calcium-sensitive dyes to assess calcium release patterns in the isolated, superfused atrium.

Use of a 4×4 pixel average for a regional measurement can, in theory, affect the upstroke delay as this area is a combination of several cardiomyocytes. Despite this, it is common practice to use a slightly higher regional area to gain signal quality. The signal to noise level does not allow automated analysis of action potential peaks at present with the information from only one pixel. The intensity of emitted light seems the major limitation inhibiting yet finer spatial and temporal resolution in the proposed setup. New optical dyes with higher optical yields may help to further improve resolution and reliability of the system (Lee et al., 2012a,b; Lee et al., 2012a,b). Local stimulation at a defined point within the atrial tissue will allow us to discern longitudinal and transverse conduction properties, and enable programmed stimulation protocols. Fixation of the tissue at the end of the experiment, which was not done in the present study, will allow us to relate regional electrophysiological changes (e.g. conduction block, or differences in action potential duration) to histological changes.

4.4. Conclusions

Using the techniques described above, murine atria but also ventricular neonatal or embryonal whole hearts may be investigated in the future, driving new insight into inborn errors leading to cardiomyopathy, heart failure and arrhythmias.

This novel technique for optical mapping and analysis of optical action potentials was developed as a tool for experimentation with murine cardiac atrial electrophysiology and will help to drive insights into how genetic changes and environmental factors influence atrial activation and repolarisation properties, thereby helping to elucidate mechanisms of atrial arrhythmias.

Funding

Preliminary data award (LF) of Research Development Fund, University of Birmingham; Engineering and Physical Sciences Research council funds the PSIBS doctoral training centre EP/F50053X/1, University of Birmingham (TY); UoB starter grant (LF, PK). BmedSci intercalation (BO, FS, LF), EUTRAF and BHF.

Editors' note

Please see also related communications in this issue by Seo et al. (2014) and Verheule et al. (2014).

Acknowledgements

We thank Genna Riley and Sarah Hopkins for help with breeding of murine models. We thank Sander Verheule, Peter Kohl and Patrizia Camelliti for advice on optical mapping techniques. Alan Race for computational and Prem Kumar for logistical support.

References

Arora, R., Verheule, S., Scott, L., Navarrete, A., Katari, V., Wilson, E., et al., 2003. Arrhythmogenic substrate of the pulmonary veins assessed by high-resolution optical mapping. Circulation 107, 1816–1821. http://dx.doi.org/10.1161/01.Cir.0000058461.86339.7e.

Bachtel, A.D., Gray, R.A., Stohlman, J.M., Bourgeois, E.B., Pollard, A.E., Rogers, J.M., 2011. A novel approach to dual excitation ratiometric optical mapping of cardiac action potentials with di-4-ANEPPS using pulsed LED excitation. IEEE Trans. Biomed. Eng. 58, 2120–2126. http://dx.doi.org/10.1109/TBME.2011.2148719.

Baker, L.C., London, B., Choi, B.-R., Koren, G., Salama, G., 2000. Enhanced dispersion of repolarization and refractoriness in transgenic mouse hearts promotes reentrant ventricular tachycardia. Circ. Res. 86, 396–407. http://dx.doi.org/10.1161/01.RES.86.4.396.

Benes, J., Ammirabile, G., Sankova, B., Campione, M., Krejci, E., Kvasilova, A., et al., 2014. The role of connexin40 in developing atrial conduction. Fed. Eur. Biochem. Sci. Lett. 588, 1465–1469. http://dx.doi.org/10.1016/j.febslet.2014.01.032.

Benjamin, E.J., Rice, K.M., Arking, D.E., Pfeufer, A., van Noord, C., Smith, A.V., et al., 2009. Variants in ZFHX3 are associated with atrial fibrillation in individuals of European ancestry. Nat. Genet. 41, 879–881. http://dx.doi.org/10.1038/ng.416.

Bezzina, C.R., Barc, J., Mizusawa, Y., Remme, C.A., Gourraud, J.-B., Simonet, F., et al., 2013. Common variants at SCN5A-SCN10A and HEY2 are associated with Brugada syndrome, a rare disease with high risk of sudden cardiac death. Nat. Genet. 45, 1044–1049. http://dx.doi.org/10.1038/ng.2712.

Blana, A., Kaese, S., Fortmuller, L., Laakmann, S., Damke, D., van Bragt, K., et al., 2010. Knock-in gain-of-function sodium channel mutation prolongs atrial action potentials and alters atrial vulnerability. Heart Rhythm 7, 1862–1869. http://dx.doi.org/10.1016/j.hrthm.2010.08.016.

Brunner, M., Kodirov, S., 2003. In vivo gene transfer of Kv1. 5 normalizes action potential duration and shortens QT interval in mice with long QT phenotype. Am. J. Physiol. Heart Circ. Physiol., 194–203, 02115.

Camm, A.J., Al-Khatib, S.M., Calkins, H., Halperin, J.L., Kirchhof, P., Lip, G.Y.H., et al., 2012a. A proposal for new clinical concepts in the management of atrial fibrillation. Am. Heart J. 164, 292–302.e1. http://dx.doi.org/10.1016/j.ahj.2012.05.017.

Camm, A.J., Lip, G.Y.H., De Caterina, R., Savelieva, I., Atar, D., Hohnloser, S.H., et al., 2012b. 2012 focused update of the ESC Guidelines for the management of atrial fibrillation: an update of the 2010 ESC Guidelines for the management of atrial fibrillation. Developed with the special contribution of the European Heart Rhythm Association. Eur. Heart J. 33, 2719–2747. http://dx.doi.org/10.1093/eurheartj/ehs253.

Di Diego, J.M., Sicouri, S., Myles, R.C., Burton, F.L., Smith, G.L., Antzelevitch, C., 2013. Optical and electrical recordings from isolated coronary-perfused ventricular wedge preparations. J. Mol. Cell. Cardiol. 54, 53–64. http://dx.doi.org/10.1016/j.yjmcc.2012.10.017.

Dou, Y., Arlock, P., Arner, A., 2007. Blebbistatin specifically inhibits actin-myosin interaction in mouse cardiac muscle. Am. J. Physiol. Cell Physiol., 1148–1153. http://dx.doi.org/10.1152/ajpcell.00551.2006.

Eckstein, J., Zeemering, S., Linz, D., Maesen, B., Verheule, S., van Hunnik, A., et al., 2013. Transmural conduction is the predominant mechanism of breakthrough during atrial fibrillation: evidence from simultaneous endo-epicardial high-density activation mapping. Circ. Arrhythm. Electrophysiol. 6, 334–341. http://dx.doi.org/10.1161/CIRCEP.113.000342.

Efimov, I., Fahy, G., 1997. High resolution fluorescent imaging does not reveal a distinct atrioventricular nodal anterior input channel (fast pathway) in the rabbit heart during sinus rhythm. J. Cardiovasc. Electrophysiol. 8, 295–306.

Efimov, I.R., Huang, D.T., Rendt, J.M., Salama, G., 1994. Optical mapping of repolarization and refractoriness from intact hearts. Circulation 90, 1469–1480.

Ehrenberg, B., Farkas, D.L., Fluhler, E.N., Lojewska, Z., Loew, L.M., 1987. Membrane potential induced by external electric field pulses can be followed with a potentiometric dye. Biophys. J. 51, 833–837. http://dx.doi.org/10.1016/S0006-3495(87)83410-0.

Ellinor, P.T., Lunetta, K.L., Albert, C.M., Glazer, N.L., Ritchie, M.D., Smith, A.V., et al., 2012. Meta-analysis identifies six new susceptibility loci for atrial fibrillation. Nat. Genet. 44, 670–675. http://dx.doi.org/10.1038/ng.2261.

Fabritz, L., Damke, D., Emmerich, M., Kaufmann, S.G., Theis, K., Blana, A., et al., 2010. Autonomic modulation and antiarrhythmic therapy in a model of long QT syndrome type 3. Cardiovasc. Res. 87, 60–72. http://dx.doi.org/10.1093/cvr/cvq029.

Fabritz, L., Fortmuller, L., Yu, T.Y., Paul, M., Kirchhof, P., 2012. Can preload-reducing therapy prevent disease progression in arrhythmogenic right ventricular cardiomyopathy? Experimental evidence and concept for a clinical trial. Prog. Biophys. Mol. Biol. 110, 340–346. http://dx.doi.org/10.1016/j.pbiomolbio.2012.08.010.

Fabritz, L., Hoogendijk, M.G., Scicluna, B.P., van Amersfoorth, S.C., Fortmueller, L., Wolf, S., et al., 2011. Load-reducing therapy prevents development of arrhythmogenic right ventricular cardiomyopathy in plakoglobin-deficient mice. J. Am. Coll. Cardiol. 57, 740–750. http://dx.doi.org/10.1016/j.jacc.2010.09.046.

Faggioni, M., Savio-Galimberti, E., Venkataraman, R., Hwang, H.S., Kannankeril, P.J., Darbar, D., et al., 2014. Suppression of spontaneous ca elevations prevents atrial fibrillation in calsequestrin 2-null hearts. Circ. Arrhythm. Electrophysiol. 7, 313–320. http://dx.doi.org/10.1161/CIRCEP.113.000994.

Fedorov, V.V., Lozinsky, I.T., Sosunov, E.A., Anyukhovsky, E.P., Rosen, M.R., Balke, C.W., et al., 2007. Application of blebbistatin as an excitation-contraction uncoupler for electrophysiologic study of rat and rabbit hearts. Heart Rhythm 4, 619–626. http://dx.doi.org/10.1016/j.hrthm.2006.12.047.

Glukhov, A., Flagg, T., Fedorov, V., 2010. Differential K ATP channel pharmacology in intact mouse heart. J. Mol. Cell. Cardiol. 48, 152–160. http://dx.doi.org/10.1016/j.yjmcc.2009.08.026.

Gudbjartsson, D.F., Arnar, D.O., Helgadottir, A., Gretarsdottir, S., Holm, H., Sigurdsson, A., et al., 2007. Variants conferring risk of atrial fibrillation on chromosome 4q25. Nature 448, 353–357. http://dx.doi.org/10.1038/nature06007.

Jou, C.J., Spitzer, K.W., Tristani-Firouzi, M., 2010. Blebbistatin effectively uncouples the excitation-contraction process in zebrafish embryonic heart. Cell. Physiol. Biochem. 25, 419–424. http://dx.doi.org/10.1159/000303046.

Kirchhof, P., Breithardt, G., Aliot, E., Al Khatib, S., Apostolakis, S., Auricchio, A., et al., 2013. Personalized management of atrial fibrillation: proceedings from the fourth Atrial Fibrillation competence NETwork/European Heart Rhythm Association consensus conference. Europace 15, 1540–1556. http://dx.doi.org/10.1093/europace/eut232.

Kirchhof, P., Kahr, P., Kaese, S., 2011a. PITX2c is expressed in the adult left atrium, and reducing Pitx2c expression promotes atrial fibrillation inducibility and complex changes in gene expression. Circ. Cardiovasc. Genet. http://dx.doi.org/10.1161/CIRCGENETICS.110.958058.

Kirchhof, P., Marijon, E., Fabritz, L., Li, N., Wang, W., Wang, T., et al., 2011b. Overexpression of cAMP-response element modulator causes abnormal growth and development of the atrial myocardium resulting in a substrate for sustained atrial fibrillation in mice. Int. J. Cardiol. http://dx.doi.org/10.1016/j.ijcard.2011.10.057.

Knollmann, B.C., Katchman, A.N., Franz, M.R., 2001. Monophasic action potential recordings from intact mouse heart: validation, regional heterogeneity, and relation to refractoriness. J. Cardiovasc. Electrophysiol. 12, 1286–1294.

Kohl, P., Hunter, P., Noble, D., 1999. Stretch-induced changes in heart rate and rhythm: clinical observations, experiments and mathematical models. Prog. Biophys. Mol. Biol. 71, 91–138. http://dx.doi.org/10.1016/S0079-6107(98)00038-8.

Laughner, J.I., Ng, F.S., Sulkin, M.S., Arthur, R.M., Efimov, I.R., 2012. Processing and analysis of cardiac optical mapping data obtained with potentiometric dyes. Am. J. Physiol. Heart Circ. Physiol. 303, H753–H765. http://dx.doi.org/10.1152/ajpheart.00404.2012.

Lee, P., Bollensdorff, C., Quinn, T.A., Wuskell, J.P., Loew, L.M., Kohl, P., 2011. Single-sensor system for spatially resolved, continuous, and multiparametric optical mapping of cardiac tissue. Heart Rhythm 8, 1482–1491. http://dx.doi.org/10.1016/j.hrthm.2011.03.061.

Lee, P., Taghavi, F., Yan, P., Ewart, P., Ashley, E.A., Loew, L.M., et al., 2012a. In situ optical mapping of voltage and calcium in the heart. PLoS One 7, e42562. http://dx.doi.org/10.1371/journal.pone.0042562.

Lee, P., Yan, P., Ewart, P., Kohl, P., Loew, L.M., Bollensdorff, C., 2012b. Simultaneous measurement and modulation of multiple physiological parameters in the isolated heart using optical techniques. Pflugers Arch. 464, 403–414. http://dx.doi.org/10.1007/s00424-012-1135-6.

Lemoine, M.D., Duverger, J.E., Naud, P., Chartier, D., Qi, X.Y., Comtois, P., et al., 2011. Arrhythmogenic left atrial cellular electrophysiology in a murine genetic long QT syndrome model. Cardiovasc. Res. 92, 67–74. http://dx.doi.org/10.1093/cvr/cvr166.

Loew, L.M., 1996. Potentiometric dyes: imagingelectrical activity of cell membranes. Pure Appl. Chem. 68, 1405–1409. http://dx.doi.org/10.1351/pac199668071405.

Mandapati, R., Skanes, A., Chen, J., Berenfeld, O., Jalife, J., 2000. Stable microreentrant sources as a mechanism of atrial fibrillation in the isolated sheep heart. Circulation 101, 194–199. http://dx.doi.org/10.1161/01.CIR.101.2.194.

Park, J., Werley, C.A., Venkatachalam, V., Kralj, J.M., Dib-Hajj, S.D., Waxman, S.G., et al., 2013. Screening fluorescent voltage indicators with spontaneously spiking HEK cells. PLoS One 8, e85221. http://dx.doi.org/10.1371/journal.pone.0085221.

Riley, G., Syeda, F., Kirchhof, P., Fabritz, L., 2012. An introduction to murine models of atrial fibrillation. Front. Physiol. 3, 296. http://dx.doi.org/10.3389/fphys.2012.00296.

Rohr, S., Salzberg, B.M., 1994. Multiple site optical recording of transmembrane voltage (MSORTV) in patterned growth heart cell cultures: assessing electrical behavior, with microsecond resolution, on a cellular and subcellular scale. Biophys. J. 67, 1301–1315. http://dx.doi.org/10.1016/S0006-3495(94)80602-2.

Salama, G., Lombardi, R., Elson, J., 1987. Maps of optical action potentials and NADH fluorescence in intact working hearts. Am. J. Physiol. 252, H384–H394.

Salzberg, B.M., Davila, H.V., Cohen, L.B., 1973. Optical recording of impulses in individual neurones of an invertebrate Central nervous system. Nature 246, 508–509. http://dx.doi.org/10.1038/246508a0.

Savitzky, A., Golay, M.J.E., 1964. Smoothing and differentiation of data by simplified least squares procedures. Anal. Chem. 36, 1627–1639. http://dx.doi.org/10.1021/ac60214a047.

Schotten, U., Verheule, S., Kirchhof, P., Goette, A., 2011. Pathophysiological mechanisms of atrial fibrillation: a translational appraisal. Physiol. Rev. 91, 265–325. http://dx.doi.org/10.1152/physrev.00031.2009.

Seo, K., Inagaki, M., Hidaka, I., Fukano, H., Sugimachi, M., Hisada, T., Nishimura, S., Sugiura, S., 2014. Relevance of cardiomyocyte mechano-electric coupling to stretch-induced arrhythmias: Optical voltage/calcium measurement in mechanically stimulated cells, tissues and organs. Prog. Bio. Mol. Biol. 115 (2-3), 129–139. http://dx.doi.org/10.1016/j.pbiomolbio.2014.07.008.

Verheule, S., Sato, T., Everett, T., Engle, S.K., Otten, D., Rubart-von der Lohe, M., et al., 2004. Increased vulnerability to atrial fibrillation in transgenic mice with selective atrial fibrosis caused by overexpression of TGF-beta1. Circ. Res. 94, 1458–1465. http://dx.doi.org/10.1161/01.RES.0000129579.59664.9d.

Verheule, S., Tuyls, E., 2013. Loss of continuity in the thin epicardial layer because of endomysial fibrosis increases the complexity of atrial fibrillatory conduction. Circ. Arrhythm. Electrophysiol., 202–211. http://dx.doi.org/10.1161/CIRCEP.112.975144.

Verheule, S., Eckstein, J., Linz, D., Maesen, B., Bidar, E., Gharaviri, A., Schotten, U., 2014. Role of endo-epicardial dissociation of electrical activity and transmural conduction in the development of persistent atrial fibrillation. Prog. Bio. Mol. Biol. 115 (2-3), 173–185. http://dx.doi.org/10.1016/j.pbiomolbio.2014.07.007.

Wakili, R., Voigt, N., Kääb, S., Dobrev, D., Nattel, S., 2011. Recent advances in the molecular pathophysiology of atrial fibrillation. J. Clin. Invest. 121, 2955–2968. http://dx.doi.org/10.1172/JCI46315.

Waldeyer, C., Fabritz, L., Fortmueller, L., Gerss, J., Damke, D., Blana, A., et al., 2009. Regional, age-dependent, and genotype-dependent differences in ventricular action potential duration and activation time in 410 Langendorff-perfused mouse hearts. Basic Res. Cardiol. 104, 523–533. http://dx.doi.org/10.1007/s00395-009-0019-1.

Wang, J., Klysik, E., Sood, S., 2010. Pitx2 prevents susceptibility to atrial arrhythmias by inhibiting left-sided pacemaker specification. Proc. Natl. Acad. Sci., 1–6. http://dx.doi.org/10.1073/pnas.0912585107.

Wu, J., Biermann, M., Rubart, M., Zipes, D.P., 1998. Cytochalasin D as excitation-contraction uncoupler for optically mapping action potentials in wedges of ventricular myocardium. J. Cardiovasc. Electrophysiol. 9, 1336–1347.

Wu, J., Olgin, J., Miller, J., Zipes, D., 2001. Mechanisms underlying the reentrant circuit of atrioventricular nodal reentrant tachycardia in isolated canine atrioventricular nodal preparation using optical mapping. Circ. Res., 1189–1195.